A Novel and General Approach for Solving the Ion-flow field Problem by a regularization technique

QiWen Cheng, Jun Zou, Stéphane Clénet

Abstract—**In order to have a better convergence and accuracy for solving the ion-flow field problem, a novel and general numerical approach is proposed. In the past, the framework of the traditional mesh based method has a dilemma that the Kapzov boundary condition can be imposed properly, and it must have two loops: the "well-posed" problem is solved in the inner loop and the secant based method is applied to impose the Kapzov assumption in the outer loop. In contrast, the proposed method solves the ion flow field problem from the perspective of the inverse problem. The original boundary value problem is transformed into a regularized optimization problem based on the prior information about the smooth ion distribution on the conductors. The objective function is separated into two parts and minimized by the alternating direction iterative method. In contrast to the traditional methods, the proposed method has removed the redundant iterations and the contentious simplifications. Numerical experiments show that the performance of the proposed method is superior to the traditional method and the results obtained by the proposed method agree better with the physical law than the traditional method. the new method presents a general and rigorous way to analysis the ion-flow field problem.**

Index Terms—**corona, space charge, HVDC transmission line, inverse problem.**

I. INTRODUCTION

THE corona discharge and the related distribution of the ion flow field are important factors for the engineering applications, such as the HVDC transmission lines or the electrostatic precipitator. The ionization layer keeps emitting charged particles to the drift region under the force of electric field. The space charge drift along in the direction defined by the ion flow field. The electric field distribution is governed by the Poisson equation and the ion flow current distribution is governed by the continuity equation. These two equations are coupled to each other leading to a nonlinear problem. In the simplified transport model, the ionization layer is modeled under the Kapzov assumption [1], which yield to impose mixed boundary conditions. To solve the boundary value problem constituted by the nonlinear partial differential equations and

the mixed boundary conditions, researchers have proposed many methods, which can be roughly divided into two categories: flux tracing methods and the mesh based methods.

The flux tracing method is firstly proposed in [2], which consists in decomposing the original problem into several ordinary differential equations under the Deutsch hypothesis. The flux tracing method has been improved in [4] by adding an extra iteration to reduce the effect of the Deutsch hypothesis. The application of the flux tracing method is limited since the diffusion of the space charge and the wind's effect cannot be taken into consideration.

The mesh based methods have been firstly proposed in [3]. Generally, these methods are iterative with two nested loops: the inner loop is applied to solve the "well-posed" boundary equations by fixed point method [5] or the Newton-Raphson method [6]; the outer loop is applied to impose the Kapzov assumption by the secant method [10-12]. It exists numerous mesh based methods, where different numerical schemes have been applied to discretize the continuity equation, such as the Method of Characteristics(MOC) [5], the upwind FEM [7], the streamline upwind Petrov-Galerkin (SUPG) method [8] and Petrov-Galerkin least square (PGLS) method [9]. The secant method applied to the outer loop, modifies the ion density on the electrode node by node. The underlying assumption of that method is that the electric field on the electrode surface is only affected by the ion density on the same node, which is also called the "injection law" [13-14] in the electrostatic precipitator models. In practice, these node by node modifications lead to unphysical results like the emission of too many ions at one point than its neighbors. To tackle this issue, several techniques have been applied in the outer loop such as the local averaging [10], the uniform distribution [7], the linear distribution [24]. These extra treatments make the results much more unpredictable [15].

Despite some spurious effects of the assumption made when solving the outer loop, the results obtained by the mesh based methods are in well agreement with the measured data on the ground level since the distribution at the ground plane is almost insensitive to the injection process [15,16]. From the

perspective of the engineering applications, the environment of the HVDC transmission lines become more and more complicated due to the construction of transmission lines and buildings in the close vicinity [17-19]. The spurious effect induced by the mesh based methods are less and less acceptable [24] because the "injection law" is not valid anymore [20]. Accurate methods to solve the spatial ion field distribution are then required.

From the theoretical point of view, the traditional mesh based methods have separated the ion flow field into two parts: One is the ion density on the inflow boundary which is determined by the Kapzov assumption; and the other is the spatial field distribution which is determined by a well-posed problem. These two parts have been totally decomposed during the iterations, which results in the fragment of the nonlinear relation between the ion density on the conductor surface and the spatial field distribution [10]. As a result, the traditional mesh based methods have a poor convergence rate.

In this paper, a novel and general approach is proposed to overcome the issue of the decomposition of the HVDC corona discharge Problem. The original problem is transformed into an optimization problem; and the alternating direction iterative method with a regularization technique is applied to minimize the objective function. The objective function is separated into two parts and minimized alternatively by the Newton method. Compared with the traditional mesh based methods, the proposed approach tries to solve the Poisson equation and the Continuity equation simultaneously instead of decomposing these two equations. The convergence property has been greatly improved as shown in different examples.

II. BOUNDARY VALUE PROBLEM OF THE ION FLOW FIELD

A. Simplifications

The following assumption are widely adopted while modeling the corona discharging phenomena [21]:

1) the drift region fully occupies the space between the conductors and ground plane.

2) Ionic mobility is constant and diffusional effects are assumed insignificant.

3) the effect of the wind has been neglected.

4) the electric field intensity on the corona conductor surface remains at the onset value.

The last assumption is so called Kapzov assumption [22]. The onset value E_{onset} is preset by Peek's empirical formula:

$$E_{\mathrm{onset}} = E_0 m\delta(1 + \frac{K}{\sqrt{r\delta}}), \qquad (1)$$

where m is the surface irregularity factor, E_0 and K represent the empirical constants: $E_0 = 33.7\mathrm{kV/cm}, K = 0.24\mathrm{cm}^{1/2}$ for the positive polarity and $E_0 = 31.0\mathrm{kV/cm}, K = 0.308\mathrm{cm}^{1/2}$ for the negative polarity, δ is the relative air density and r is the conductor radius.

B. Governing equations

For the sake of simplicity, the discussion in this paper has been limited to the unipolar situation. The Poisson-Continuity coupled system is as follows:

$$\begin{cases} \Delta\varphi = -\rho / \epsilon_0, \\ \nabla \cdot \boldsymbol{J} = 0 \end{cases}, \qquad (2)$$

where the $\varphi(\mathrm{V})$ represents the electric potential, $\rho(\mu\mathrm{C})$ is the space charge density, $\epsilon_0(8.85 \times 10^{-12}\mathrm{F/m})$ is the vacuum permittivity. $\boldsymbol{J}(\mu\mathrm{A/m}^2)$ is the ion flow current:

$$\boldsymbol{J} = \boldsymbol{V}\rho \qquad (3)$$

where $\boldsymbol{V}(\mathrm{m/s})$ is the velocity of the ion. It is proportional to the electric field:

$$\boldsymbol{V} = \mu\boldsymbol{E} \qquad (4)$$

where $\mu(1.5 \times 10^{-4}\mathrm{m}^2/(\mathrm{V}\cdot\mathrm{s}))$ represents the ion mobility.

C. Boundary conditions

The general configuration of the unipolar wire-plate model is shown in fig. 1. The surface of the electrode is denoted Γ_c, the ground Γ_g and the remaining artificial rectangle boundary Γ_a.

The electric potential on the electrode surface is equal to the applied voltage and the potential on the artificial boundary is set as the Laplacian field. So the boundary conditions for the Poisson equation is as follows:

$$\begin{cases} \varphi = \varphi_{\mathrm{applied\,voltage}}, & \boldsymbol{x} \in \Gamma_c \\ \varphi = 0, & \boldsymbol{x} \in \Gamma_g \\ \varphi = \varphi_{\mathrm{Laplacian}}, & \boldsymbol{x} \in \Gamma_a \end{cases} \qquad (5)$$

The boundary condition for the Continuity equation is as follows:

$$E(\boldsymbol{x}) = E_{\mathrm{onset}}, \quad \boldsymbol{x} \in \Gamma_c \qquad (6)$$
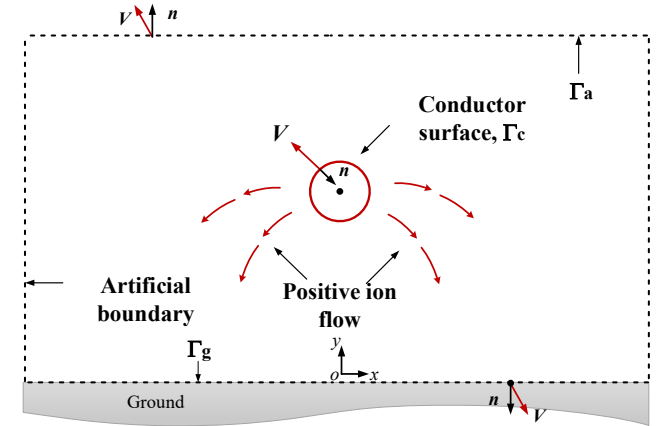

Fig. 1. Configuration of the unipolar wire-plate model.

III. REGULARIZED OPTIMIZATION PROBLEM

In this section, the original boundary value problem is discretized leading to a nonlinear algebraic equation firstly. Then the algebraic equation is transformed to an optimization problem with a regularization term.

A. Nonlinear Algebraic Equations

First of all, the nonlinear partial differential equations (2) are transformed into a set of nonlinear algebraic equations by applying the Galerkin method [6]. The ion density and the electric potential are expressed as a linear combination of the quadratic basis functions $\{N_i(\boldsymbol{x})\}$:

$$\rho_h = \sum_{i=1}^{n} \rho_i N_i(\boldsymbol{x}), \quad \varphi_h = \sum_{i=1}^{n} \varphi_i N_i(\boldsymbol{x}) \qquad (7)$$

where φ_i and ρ_i represent the nodal value of φ and ρ at the node i. The weak form of the original partial differential equations is [6]:

$$\begin{cases} R_i^\rho = \left\langle \nabla \cdot (V\rho_h), N_i + \dfrac{V}{2\|V\|} \cdot \nabla N_i \right\rangle = 0, \quad i = 1,2,\cdots n \\ R_i^\varphi = \left\langle \Delta\varphi_h + \dfrac{\rho_h}{\epsilon_0}, N_i \right\rangle = 0, \quad i = 1,2,\cdots n \end{cases} \qquad (8)$$

where $<\cdot>$ represents the integral over the domain. The Poisson equation is discretized by the Galerkin method and the corresponding residual on the node i is represented by R_i^φ. The Continuity equation is discretized by the streamline upwind method (SUPG) and the corresponding residual is represented by the R_i^ρ.

In order to impose the Dirichlet boundary conditions (5), we have added the following residual equations to the one related to the residual R_i^φ introduced in (8):

$$\begin{cases} R_i^\varphi = \varphi_i - \varphi_{\text{applied voltage}} = 0, \quad i \in A_c \\ R_i^\varphi = \varphi_i = 0, \quad i \in A_g \\ R_i^\varphi = \varphi_i - \varphi_{\text{Laplacian}} = 0, \quad i \in A_a \end{cases} \qquad (9)$$

where the sets A_c, A_g and A_a represent the nodes on the Γ_c, Γ_g and Γ_a respectively. In the same way, additional equations are added to account for the boundary condition (6) to the residual equations (8) related to the terms R_i^ρ :

$$R_i^\rho = E_i - E_{on} = -\nabla_h\varphi - E_{\text{onset}} = 0, \quad i \in A_c \qquad (10)$$

where ∇_h represents the numerical differential operator.

Discretized with the Galerkin method and the SUPG method, the original nonlinear partial differential equations (2) and the boundary condition (5) have been transformed to the following nonlinear algebraic equations:

$$\boldsymbol{R}(\boldsymbol{u}) := \begin{pmatrix} \boldsymbol{R}^\rho \\ \boldsymbol{R}^\varphi \end{pmatrix} = \boldsymbol{0} \qquad (11)$$

where the unknown variable $\boldsymbol{u}$ and the residual vectors $\boldsymbol{R}^\varphi, \boldsymbol{R}^\rho$ are defined as follows:

$$\begin{cases} \boldsymbol{u} = (\rho_1, \rho_2, \cdots \rho_n, \varphi_1, \varphi_2, \cdots \varphi_n)^T \\ \boldsymbol{R}^\varphi = (R_1^\varphi, R_2^\varphi, \cdots R_n^\varphi)^T \\ \boldsymbol{R}^\rho = (R_1^\rho, R_2^\rho, \cdots R_n^\rho)^T \end{cases} \qquad (12)$$

B. Optimization Problem

The Dirichlet boundary conditions (5) and Neumann boundary condition (6) have to be imposed on the conductor boundary simultaneously, which results in ill conditioned nonlinear equations (11) [23]. To overcome this issue, we propose to consider the original problem as an inverse problem [26]. The onset electric field on the conductor surface is considered as the "measured data". The ion density on the conductor surface is the model parameter, which should be reconstructed from the measured data. The residual vector $\boldsymbol{R}$ (11) and the unknown vector $\boldsymbol{u}$ (12) are divided into two parts:

$$\begin{cases} \boldsymbol{R}_1(\boldsymbol{u}_1, \boldsymbol{u}_2) = \boldsymbol{0} \\ \boldsymbol{R}_2(\boldsymbol{u}_1, \boldsymbol{u}_2) = \boldsymbol{0} \end{cases}, \qquad (13)$$

where $\boldsymbol{u}_1$ represents the ion density on the conductor surface and $\boldsymbol{u}_2$ represents the other spatial field. The corresponding residual equations of $\boldsymbol{u}_1$ is represented by $\boldsymbol{R}_1$ and $\boldsymbol{R}_2$ represents the residual equations related to $\boldsymbol{u}_2$. From the perspective of the inverse problem, the residual $\boldsymbol{R}_1$ represents the deviation between the target electric field intensity E_{onset} and the actual electric field calculated from the field distribution $\boldsymbol{u}_2$, which is also called the data error. The residual $\boldsymbol{R}_2$ represents the error of the numerical Poisson-Continuity system, which is also called the model error. The original nonlinear algebraic equation (11) is transformed to the an optimization problem:

$$\boldsymbol{u} = \operatorname{argmin} \| \boldsymbol{R}_1(\boldsymbol{u}_1, \boldsymbol{u}_2) \|_2^2 + \| \boldsymbol{R}_2(\boldsymbol{u}_1, \boldsymbol{u}_2) \|_2^2 \qquad (14)$$

where $\| \cdot \|_2$ represents the standard 2-norm and "argmin" is the abbreviation of "find the argument $\boldsymbol{u}_1$ and $\boldsymbol{u}_2$ that minimizes the following objective function".

The optimization problem (14) cannot be solved directly since the ill-posed property of this problem still remains since the system of equations has been rearranged (from (11) to (13)) but not modified. The ion density on the conductor surface is sensitive to the electric field that a small disturbance of the electric field will result in a local spurious ion density distribution with high ripples. In order to reduce the ion density distribution sensitivity, a regularization term has been added to the objective function and the initial problem (14) becomes:

$$\boldsymbol{u} = \operatorname{argmin} \| \boldsymbol{W}_d \boldsymbol{R}_1(\boldsymbol{u}_1, \boldsymbol{u}_2) \|_2^2 + \alpha T(\boldsymbol{u}_1) + \| \boldsymbol{R}_2(\boldsymbol{u}_1, \boldsymbol{u}_2) \|_2^2 \ (15)$$

where the normalized matrix is defined as $\boldsymbol{W}_d = \operatorname{diag}(E_{\text{onset}}, E_{\text{onset}}, \cdots E_{\text{onset}})$. The coefficient α represents the regularization factor and $T(\boldsymbol{u}_1)$ is the generalized Tikhonov regularization term, which is defined as follows:

$$T(\boldsymbol{u}_1) = \| \boldsymbol{W}_m \boldsymbol{u}_1 \|_2^2 \qquad (16)$$

where the corresponding smoothing matrix $\boldsymbol{W}_m$ is defined as follows:

$$\boldsymbol{W}_m = \begin{pmatrix} 1/h & -1/h & 0 & \cdots & \cdots \\ 0 & 1/h & -1/h & 0 & \cdots \\ \vdots & \vdots & \vdots & \vdots & \vdots \\ \cdots & \cdots & 0 & 1/h & -1/h \\ -1/h & 0 & \cdots & 0 & 1/h \end{pmatrix}, \qquad (17)$$

where h is the distance between the adjacent nodes on the conductor surface. The matrix $\boldsymbol{W}_m$ can be considered as the first order finite difference operator so the regularization term $T(\boldsymbol{u}_1)$ in (16) is applied in order to minimize the space variability of the ion density distribution on the conductor surface.

IV. METHOD PRESENTATION

From the perspective of the inverse problem theory, the original problem is equivalent to reconstruct the ion density on the conductor surface from the electric field intensity on the conductor surface:

$$\text{find } \boldsymbol{u}_1 \text{ by minimizing } \| \boldsymbol{W}_d \boldsymbol{R}_1(\boldsymbol{u}_1, \boldsymbol{u}_2) \| + \alpha T(\boldsymbol{u}_1) \qquad (18)$$

The corresponding forward problem is defined as follows:

find u_2 by solving: $R_2(u_1, u_2) = 0$ (19)

In the definition (19), the ion density on the conductor surface, which is represented by u_1, is already known and the unknown variable is the spatial field distribution, which is represented by u_2.

The objective function (15) is composed of the inverse problem (18) and the forward problem (19). In the presented work, the alternating direction iterative method is applied to solve these two parts respectively [29]. The details of the algorithm are shown in the following subsections.

A. Update of u_1

In this part, the unknown vector u_1 is updated by minimizing the following residual in one step:

$$u_1 = \arg\min \| W_d R_1(u_1, u_2) \|_2^2 + \alpha T(u_1) \qquad (20)$$

The residual R_1 with the regularization term is linearized as follows:

$$\begin{aligned} \| W_d R_1(u^{(k+1)}) \|_2^2 + \alpha T(u_1^{(k+1)}) \approx \\ \| W_d R_1(u^{(k)}) \|_2^2 + \alpha T(u_1^{(k)}) + 2g_1^T \delta u_1 + \delta u_1^T G_1 \delta u_1 \end{aligned} \qquad (21)$$

where the vector g_1 and the coefficient matrix G_1 are:

$$g_1 = H^T W_d R_1 + \alpha W_m^T W_m u_1, \quad G_1 = H^T H + \alpha W_m^T W_m, \quad (22)$$

and the coefficient matrix H is defined as follows:

$$H = W_d \left(\frac{\partial R_1}{\partial u_1} + \frac{\partial R_1}{\partial u_2} \frac{\partial u_2}{\partial u_1} \right) \qquad (23)$$

The unknown variables u_2 can be considered as the function of the u_1 and the first order derivative can be obtained from the implicit differentiation method:

$$\frac{\partial u_2}{\partial u_1} = -\left(\frac{\partial R_2}{\partial u_2} \right)^{-1} \frac{\partial R_2}{\partial u_1} \qquad (24)$$

The increment δu_1 to u_1 is determined by cancelling the residual (21) leading to:

$$\delta u_1 = -G_1^{-1} g_1 \quad u_1^{(k+1)} = u_1^{(k)} + \delta u_1 \qquad (25)$$

B. Update of u_2

In this part, the unknown vector u_2 is updated by minimizing the following residual in one step:

$$u_2 = \arg\min \| R_2(u_1, u_2) \|_2^2 \qquad (26)$$

The residual term R_2 is linearized as follows:

$$\begin{aligned} \| R_2(u_1^{(k+1)}, u_2^{(k+1)}) \|_2^2 \approx \| R_2(u_1^{(k+1)}, u_2^{(k)}) \|_2^2 \\ + 2g_2^T \delta u_2 + \delta u_2^T G_2 \delta u_2 \end{aligned} \qquad (27)$$

where the vector g_2 and coefficient matrix G_2 are defined as follows:

$$g_2 = \left(\frac{\partial R_2}{\partial u_2} \right)^T R_2(u_1^{(k+1)}, u_2^{(k)}), \quad G_2 = \left(\frac{\partial R_2}{\partial u_2} \right)^T \frac{\partial R_2}{\partial u_2} \qquad (28)$$

The increment δu_2 to u_2 is found by minimizing (27):

$$\delta u_2 = -G_2^{-1} g_2, \quad u_2^{(k+1)} = u_2^{(k)} + \delta u_2 \qquad (29)$$

C. Procedure

The procedure to obtain the solution of (15) with a given regularization factor α contains the following steps:

Step 1. k=0, give the initial value u^k and calculate the normalized residuals:

$$\begin{cases} r_1^{(k)} = \| W_d R_1(u_1^{(k)}, u_2^{(k)}) \|_2 / \| W_d R_1(0,0) \|_2 \\ r_2^{(k)} = \| R_2(u_1^{(k)}, u_2^{(k)}) \|_2 / \| R_2(0,0) \|_2 \end{cases} \qquad (30)$$

Step 2. Calculate the coefficient matrix H_i, G_i and the vector g_i ($i = 1,2$)

Step 3. Update u_1 as follows:

$$u_1^{(k+1)} = u_1^{(k)} + \delta u_1 \qquad (31)$$

Step 4. Update u_2 as follows:

$$u_2^{(k+1)} = u_2^{(k)} + \delta u_2 \qquad (32)$$

Step 5. Update the normalized residuals $r_1^{(k+1)}, r_2^{(k+1)}$ in (30).

Step 6. If the normalized residuals have not converged, then k=k+1, move back to step 2, otherwise, breakout the iteration.

D. Determination of the regularization factor

The objective function (20) has two terms: the data error R_1 and the regularization term $T(u_1)$. The regularization term is applied to smoothen the ion density distribution on the conductors. If the regularization factor is too small, the convergence will be unstable since we are close to the initial problem which is ill posed. If the regularization term's weight is too large, the corresponding numerical results will be a constant and it cannot reflect the property of the original Poisson-Continuity coupled system. The definition of the regularization factor is problem dependent and it is difficult to find a general approach to find it. A recommended scheme is to determine the value of α dynamically that is to say by modifying the regularization factor α depending on the coefficient matrices:

$$\alpha = \frac{\text{trace}(H^T H)}{\text{trace}(W_m^T W_m)} \qquad (33)$$

The dynamic scheme determines the factor by the ratio of two matrices' traces, which can be considered as the ratio of the sum of these matrices' eigenvalues [27].

In practical applications, the proper magnitude order of α is much more important than the exact value of α and the value generated by (33) can be a good guideline to find an order of α. For the sake of simplicity, the stationed scheme is applied in the studied cases since it is easier to show the effect of different regularization factors and the corresponding performance of the proposed method.

E. Comparison between the proposed method and the traditional mesh based methods

In the proposed method, the ion flow field problem is solved as an inverse problem. In contrast, the traditional method chooses to decompose the ill-posed problem into a series of well posed problems by setting the ion density distribution on the boundary u_1 as an artificial value. In the inner loop, the non-boundary variables u_2 is calculated by solving a well-posed boundary value problem. In the outer loop, the boundary variables u_1 is updated by imposing the Kapzov assumption.

To make a link with proposed method describing in the previous sections, the basic framework of the traditional method is rewritten under the inverse problem theory:

1. In the traditional method, the inner loop is applied to find the spatial field distribution u_2 by solving the following problem with the boundary variable u_1 known:

$$R_2(u_1, u_2) = 0 \qquad (34)$$

The equation (34) is equivalent to the optimization problem (26)

2. In the traditional method, the outer loop is applied to update the boundary variables u_1 depending on the Kapzov assumption. The most popular relations are as follows [10]:

$$\delta u_{1,j} = \frac{u_{1,j}^{(k)}}{E_j^{(k)} + E_{onset}}(E_j^{(k)} - E_{onset}) \qquad (35)$$

$$\delta u_{1,j} = \frac{u_{1,j}^{(k-1)} - u_{1,j}^{(k)}}{E_j^{(k)} - E_j^{(k-1)}}(E_j^{(k)} - E_{onset}) \qquad (36)$$

These two relations can be summarized into a general formula:

$$\delta u_1 = -\tilde{G}_1^{-1} R_1(u^{(k)}) \qquad (37)$$

where $\tilde{G}_1$ is a diagonal matrix. The relation (37) can be considered as the special case of (25) where the regularization factor α is zero and the matrix G_1 has been reduced to a diagonal matrix $\tilde{G}_1$. In the first order relation (35), the diagonal entries of $\tilde{G}_1$ are generated from the last step's result and the second order relation (36) has applied the last two steps' results to generate the matrix $\tilde{G}_1$.

The traditional method is rewritten into two optimization problems: the spatial field u_2 is updated by minimizing the model error R_2 and the boundary ion density u_1 is updated by minimizing the data error R_1. As we can see, the traditional method is similar to the proposed method, but is has the following inconvenient: the inner loop applied to solve the optimization problem (26) is meaningless and time-consuming since the solution u_2 changes as the boundary value u_1 changes; the modification in the outer loop has simplified the entries of the matrix G_1 into a diagonal matrix, which results to unphysical results; the entries of matrix $\tilde{G}_1$ are generated from a finite difference method which leads to an approximation of the real derivatives (quasi-Newton method) resulting in a slow convergence. In the proposed method, these drawbacks are solved separately:

1. The alternation direction iterative method is applied to minimize (20) and (26). The inner loop and the outer loop in the traditional method have been combined and the corresponding computational time is significantly reduced.

2. The matrix G_1 is generated from the analytical formula (23). The effect of the diagonal simplification has been removed. Furthermore, the analytical coefficient matrix G_1 results in a faster convergence than the traditional method.

3. The regularization term imposes a smooth distribution constraint based on the prior information. The solution space of the optimization problem has been significantly reduced, which facilitates the convergence.

V. APPLICATION IN PRACTICAL MODEL

In this section, the proposed method is applied to a single conductor model, a multi-conductor model and the DC experimental line model separately. The normalized residuals (30) during the iterations is displayed firstly. Then the ion density obtained by the proposed method is compared with the traditional mesh based method and the measured data or the analytical solution when available to evaluate the accuracy of the proposed method. All the computations are made on a laptop with an Intel® Core™ i7 at 2.8 GHz and 8 G memory under Matlab platform. The comparison in terms of the computational time is also presented to prove that the proposed method performances are better than the traditional method.

A. Concentric wire-cylinder model

The concentric wire-cylinder model has an analytical solution [2]. The diameter of the wire and the outer cylinder are 3mm and 0.8m respectively. The applied voltage on the wire is 90kV and the roughness factor m in (1) is 0.6. This model is applied to investigate the influence of the regularization factor and also the accuracy of the results obtained by the proposed method by comparing with the analytical result. For the sake of simplicity, the factor α has a fixed value during the iteration and several specific values of α are tested.

The effect of the regularization term is investigated firstly. The eigenvalues of matrix G_1 for different regularization factor values α are compared in fig. 2. The eigenvalues are normalized by setting the minimum eigenvalue to 1. The conditional number of G_1 without regularization term is about 10^9 and the eigenvalues decrease quickly, which indicates that the problem is ill-posed. In contrast, the conditional number of the matrix G_1 with the regularization term has been significantly reduced: the conditional number is equal to 10^2 with $\alpha = 1$ and the distribution of the eigenvalues is much uniform than before. From the numerical point of view, the regularization term has "filtered" the small eigenvalue of matrix G_1 and has stabilized the iterative process. In fact, the residuals displayed in Fig. 3 shows that the proposed method without regularization term becomes unstable after 5 iterations.
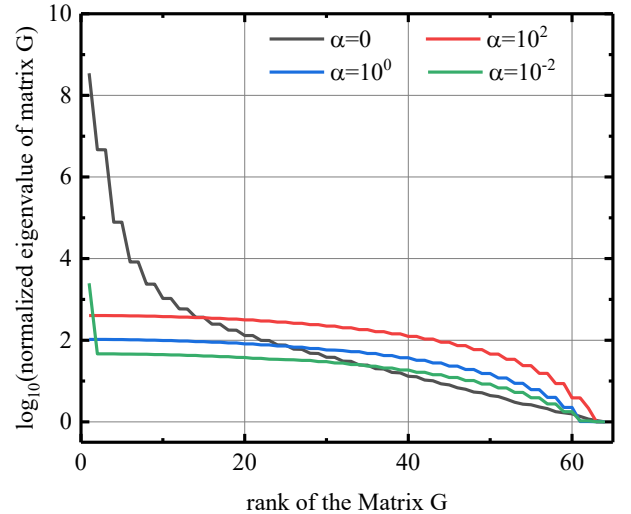

Fig. 2. Normalized eigenvalue of the Jacobian matrix under different regularization coefficients.

The normalized residuals during the iterations are compared in Fig. 3. As shown in Fig. 3(a), the normalized residual r_1 has the same behavior with different regularization factors $\alpha = 10^{-2}, 10^0, 10^2$. A possible reason is that the prior information imposed by the regularization term is completely correct in this axisymmetric model that the analytical ion density on the conductor surface happens to be a constant. The weight of the

regularization term does not affect the residuals. The performance of the proposed method is superior to the traditional method as the normalized residual r_1 of the proposed method decreases to 3×10^{-3} within 8 iterations. In contrast, the traditional method takes 14 iterations in the outer loop to reduce the residual r_1 to the same level. The normalized residual r_2 under different factors are shown in fig. 3(b). In the current model, the residuals have the same distributions and converges to 10^{-15} after 13 iterations.
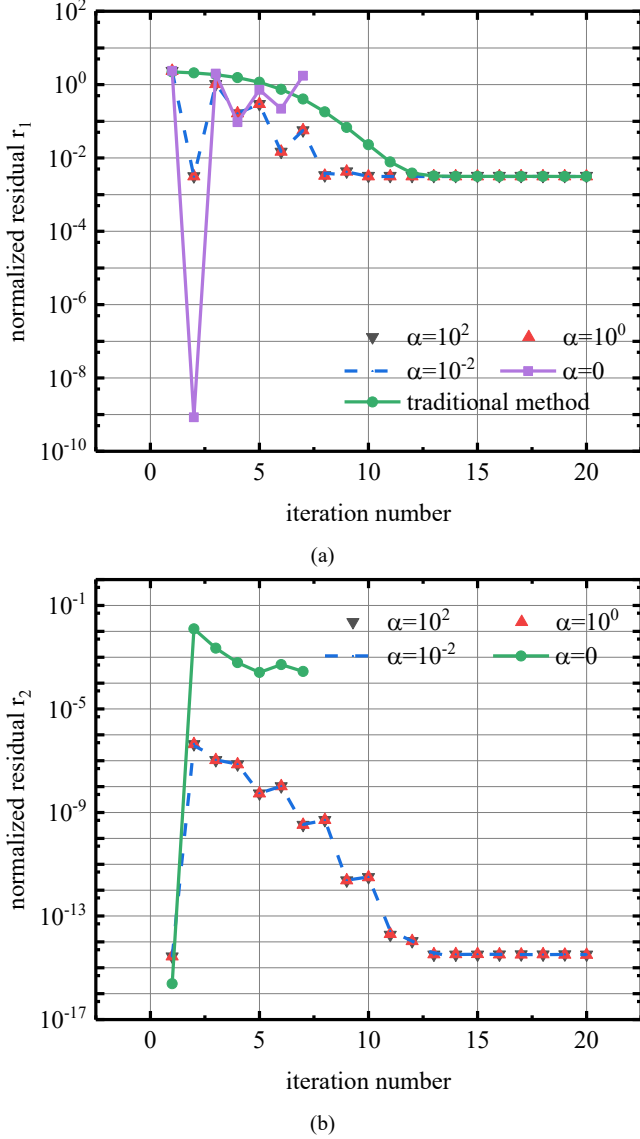

(a)

(b)

Fig. 3. (a)normalized residual r_1 during the iteration. (b) normalized residual r_2 during the iteration.

As analyzed in the last section, the calculation of the increments (31) and (32) are based on an analytical expression of the entries of the matrix $\boldsymbol{G}_1$, which leads to a faster convergence than the quasi-Newton method applied in the traditional method. Furthermore, an iteration in the proposed method involves less operations than in the traditional method since the inner loop has been simplified. As a result, the proposed method is able to reduce the computational time significantly: a single iteration in the proposed methods requires about 5.4s and the computational time of 8 iterations is

about 43.2s. In contrast, a single iteration in the outer loop of the traditional mesh based method requires about 12.5s and corresponding computational time after 14 iterations is 175s, which is about 4 times more than the proposed method.

The ion density distribution on the conductor surface obtained by two methods are compared with the one given by the analytical model in Fig. 4. In the proposed method, a large regularization factor results in a smooth ion density distribution: the distribution obtained with $\alpha = 10^2$ is almost a constant ,which is very closer to the distribution given by the analytical model. In contrast, the node by node modification applied in the traditional method has neglected all the field generated by the neighboring space charges and this scheme results in the spurious distribution with too many unphysical ripples.
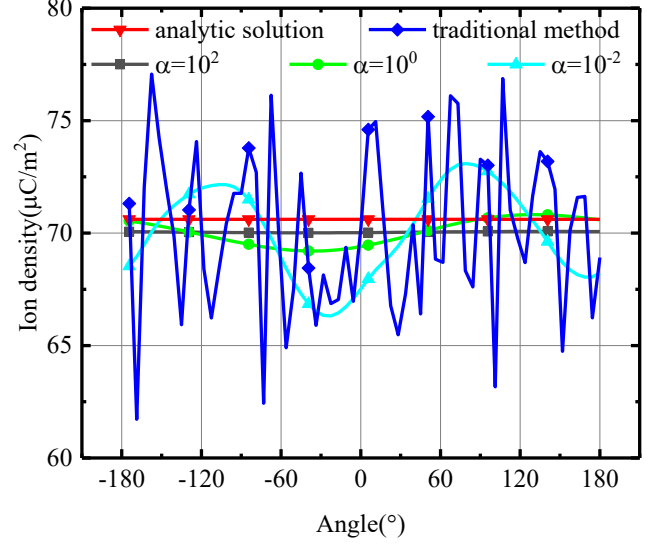

Fig. 4. Comparison of the ion density under different regularization coefficients.

B. The bundle conductor model

In this subsection, the proposed method is applied to a complex model with three conductors. The pole spacing is 14.8cm, the surface irregularity factor in this model is still 0.6 and the applied voltage on the conductors is +90kV. The results obtained by the traditional mesh based method and the proposed method are compared with the measured data [24, 25].

The dynamic scheme (33) is applied to find the proper regularization factor under this complex configuration. As shown in the Fig. 5, during the iterative process, the value of (33) converges to the fixed value 2.7×10^{-2} after 6 iterations, which is the recommended regularization factor. In the following experiment, we have compared the performance of the recommended value and the other values such as $\alpha = 10^{-4}, 10^0, 10^2$ to verify the proposed scheme.

In this example, the ion density distribution on the conductor surface is not a constant and the regularization term is not zero in this configuration. The deviation between the original optimization problems (14) and the regularized optimization problem (15) is proportional to the regularization factor and a large factor results in a large normalized residual r_1. As compared in the fig. 6: the normalized residual r_1 converges to

5×10^{-2} with $\alpha = 10^0$ and it is reduced to 2×10^{-3} with the recommended factor. The residual of the traditional method decreases in a much slower way and the final residual is still 2.5×10^{-2} after 20 iterations.
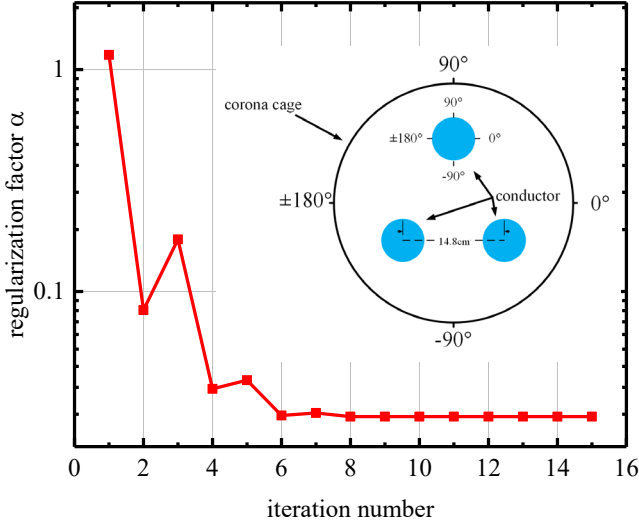

Fig. 5. The regularization factor α determined by the formula (33) during the iterations.

The normalized residual r_2 under different factors are compared in Fig. 6(b). The normalized residual r_2 with $\alpha = 10^2$ has decreased to 10^{-14} after 12 iterations, and the residual with $\alpha \in (10^0, 10^{-4})$ converges to 10^{-10}. The possible reason for this difference is that the large variation in the ion density distribution on the conductor surface results in the numerical oscillation and part of the spatial ion density is negative numerically. The authors set the negative density to zero during the iterations and this non-negative constraint may result in the large residual. Even though different regularization factors result in different r_2, the absolute value of normalized residual r_2 is much smaller than the normalized residual r_1, which means the value of the objective function (15) is dominated by the normalized residual r_1. Considering the residual r_2 is less important in the iteration process, the suitability of the regularization factor is verified from the perspective of the residual r_1 and the ion distribution on the conductor surface in the following experiment.

The ion density distributions on the top conductor surface obtained by the proposed method with different regularization factors are compared in Fig. 7. As the regularization factor decreasing to 10^{-4}, the ion density obtained from the proposed method has an oscillated distribution since the effect of the regularization term become weak. In contrast, the ion density obtained by the proposed method with $\alpha = 10^2$ is almost a constant since the weight of the regularization term is too large that the optimization problem (15) is far from the original problem. The corresponding numerical result cannot reflect the practical non-uniform field distribution around the bundle conductors. The results with the recommended value has the best performance because the numerical result on the conductor surface satisfy the smooth constraint and the Kapzov assumption simultaneously. The ion density on the conductor

surface has a smooth distribution and the density varies from $0\mu C/m^2$ to $80\mu C/m^2$. In contrast, the node by node modification in the traditional method results in the unphysical discontinuous distribution on the conductors and the ion density obtained from the traditional mesh based method varies from $20\mu C/m^2$ to $70\mu C/m^2$.

The spatial distribution of the ion density obtained from the proposed method and the traditional method is compared in fig. 8(a) and fig. 8(b). Generally, the distribution looks like the "flower" with one "petal" corresponding to one conductor [24]. The results obtained by the proposed method has distinguishable boundaries of the "petals" and the distribution obtained by the traditional method is more uniform than the proposed method. To further verify the spatial distribution obtained by the proposed method, the angular corona current distributions on the cylindrical boundary are compared with the measured data in fig. 8(c). The corona current obtained by the proposed method has a much larger angular variation, which is closer to the measured data. In contrast, the uniform spatial distribution obtained by the traditional mesh based method cannot capture the peak value and the valley value exactly.

In this example, the proposed method also is more efficient than the traditional method. A single iteration of the proposed method requires around 14s. The proposed method converges in 10 iterations and the corresponding computational time is about 140s. In contrast, a single iteration in the outer loop of the traditional mesh based method leads to a computational time is about 30s. The total computational time after 20 steps' iterations is 600s, which is about 4 times more than the proposed method.

C. DC experimental line model

To further verify the validity of the proposed method in the practical HVDC transmission line model, the proposed method is applied to a reduced-scale DC experimental line with the neighboring building. The height of the conductors to the ground is 2.1m and the distances between two poles is 2.2m. The building model made of iron sheet is 4 m away from the middle of the two poles. The surface irregularity factor is 0.52 and the applied voltage on the conductors is $\pm 100kV$. In the practical experiment, several field mills are placed to measure the electric field on the ground and on the top of the building. The details of the configuration can found in [28].

As shown in Fig. 9, the recommended value of equation (33) converges to 1.1×10^4 .The electric field intensity on the ground and the top of the building are compared with the measured data in Fig. 10. The result obtained by the traditional method is larger than the actual value and the calculated electric field on the top of the building is approximately twice the measured value. In contrast, the result obtained by the proposed method with the recommended regularization factor shows a good agreement with the measured data, the validity of the proposed method is verified.

VI. CONCLUSION

In this paper, the ion flow field problem is considered as an inverse problem. The Kapzov assumption is applied to

8

reconstruct the ion density distribution on the conductor surface. By transforming the original problem into a regularized optimization problem, the proposed method solves the ill-posed problem in a much straightforward manner. It has simplified the two loops into one and the corresponding computational time has been reduced by 4 times as show in the numerical experiments. Furthermore, the simplification or the assumptions applied in the traditional mesh based method has all been waived and the proposed method is able to capture more details of the spatial ion density distribution.

The proposed method is a general way to treat the nonlinear coupled systems with the mixed boundary conditions, which can be extended to the other applications as well.
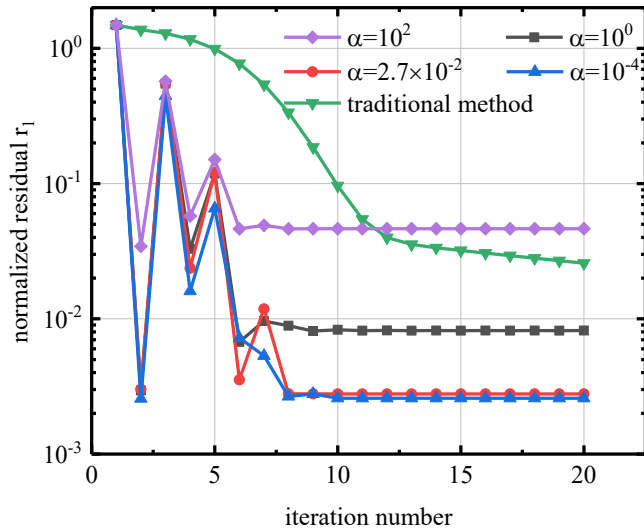
(a)
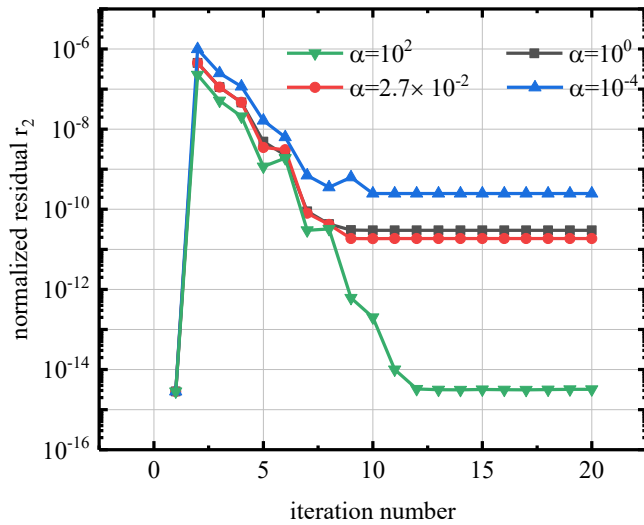
(b)

Fig. 6. (a)normalized residual r_1 during the iterations. (b) normalized residual r_2 during the iterations.

REFERENCES

[1] M. P. Sarma, "Analysis of corona losses for DC transmission line configurations" Ph.D. dissertation, Dept. Elect. Eng., University of Toronto, Canada, 1968.
[2] M. P. Sarma and W. Janischewskyj, "Analysis of Corona Losses on DC transmission Lines: I-Unipolar Lines", IEEE Trans. Power App. Syst., vol. 88, no. 5, pp. 718-731, May. 1969.
[3] W. Janischewskyj and G. Gela, "Finite element solution for electric fields of coronating DC transmission lines", IEEE Trans. Power App. Syst., vol. 98, no. 3, pp. 1000-1012, May. 1979.
[4] J. Qiao, P. Zhang, J. Zhang, Y. Lu, J. Zou, J. Yuan, and S. Huang, "An iterative flux tracing method without Deutsch assumption for ion-flow field of AC/DC hybrid transmission lines", IEEE Trans. Magn. vol. 54, no. 3, Mar. 2018.
[5] J.L. Davis and J.F. Hoburg, "HVDC transmission line computations using finite element and characteristics methods", J. Electrostat. vol. 18, pp. 1-22, 1986.
[6] J. Q. Feng, "Application of Galerkin Finite Element Method with Newton Iterations in Computing Steady-State Solutions of Unipolar Charge Currents in Corona Devices", J. Comp. Phys. vol. 151, pp. 969-989, 1999.
[7] T. Takuma, T. Ikeda and T. Kawamoto, "Calculation of Ion Flow Fields of HVDC Transmission Lines by the Finite Element Method", IEEE Trans. Power App. Syst. vol. 100, no. 12, pp. 4802-4810, Dec. 1981.
[8] J. Liu, J. Zou, J. Tian and J. Yuan, "Analysis of electric field, ion flow density, and corona loss of same-tower double circuit HVDC lines using improved FEM", IEEE Trans. Power Del. vol. 24, no. 1, pp. 482-483, 2009.
[9] J. Qiao, J. Zou, J. Zhang, Y. Lu, J. Lee and M. Ju, "Ion-flow field calculation of HVDC overhead lines using a high-order stabilization technique based on Petrov-Galerkin method", IET Gen. Trans. Dis. vol. 12, no. 5, pp. 1183-1189, 2018.
[10] T. Guillod, M. Pfeiffer and C. M. Franck, "Improved Coupled Ion-Flow Field Calculation Method for AC/DC Hybrid Overhead Power Lines", IEEE Trans. Power Del. vol. 29, no. 6, pp. 2493-2501, Dec. 2014.
[11] Z. M. Al-Hamouz, "A combined Algorithm Based on Finite Elements and a Modified Method of Characteristics for the Analysis of the Corona in Wire-Duct Electrostatic Precipitators", IEEE Trans. Ind. App. vol. 38, no. 1, pp. 43-49, Jan. 2002.
[12] H. Yin, J. He, B. Zhang and R. Zeng, "Finite Volume-Based Approach for the Hybrid Ion-Flow of UHVAC and UHVDC Transmission Lines in Parallel", IEEE Trans. Power. Del. vol. 26, no. 4, pp. 2809-2820, Oct. 2011.
[13] B. Khaddour, P. Atten and J.L. Coulomb, "Numerical solution of the corona discharge problem based on mesh redefinition and test for a charge injection law", J. Electrostat. vol. 66, pp. 254-262, Feb. 2008.
[14] B. Khaddour, P. Atten and J.L. Coulomb, "Electrical Field Modified by Injected Space Charge in Blade-Plate Configuration", IEEE Trans. Magn. vol. 42, no. 4, pp. 651-654, Apr. 2006.
[15] J.R. Li and H. J. Wintle, "Unipolar corona space charge in wire-plane geometry: A first principles numerical computation", J. Appl. Phys. vol. 65, no. 12, pp. 4617-4624, Jun. 1989.
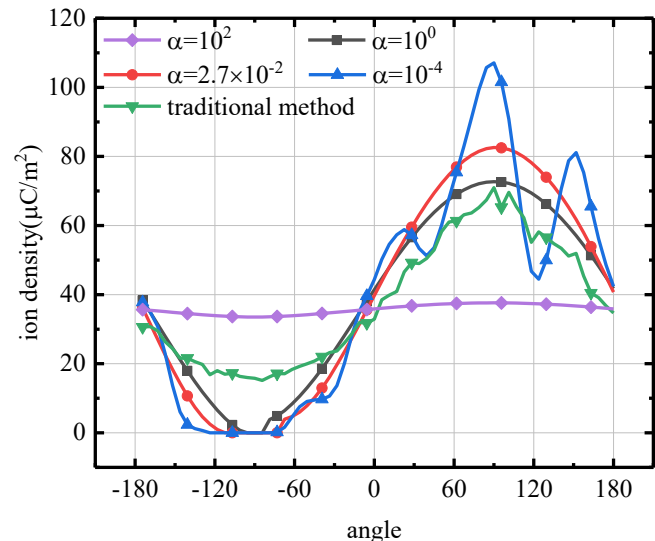
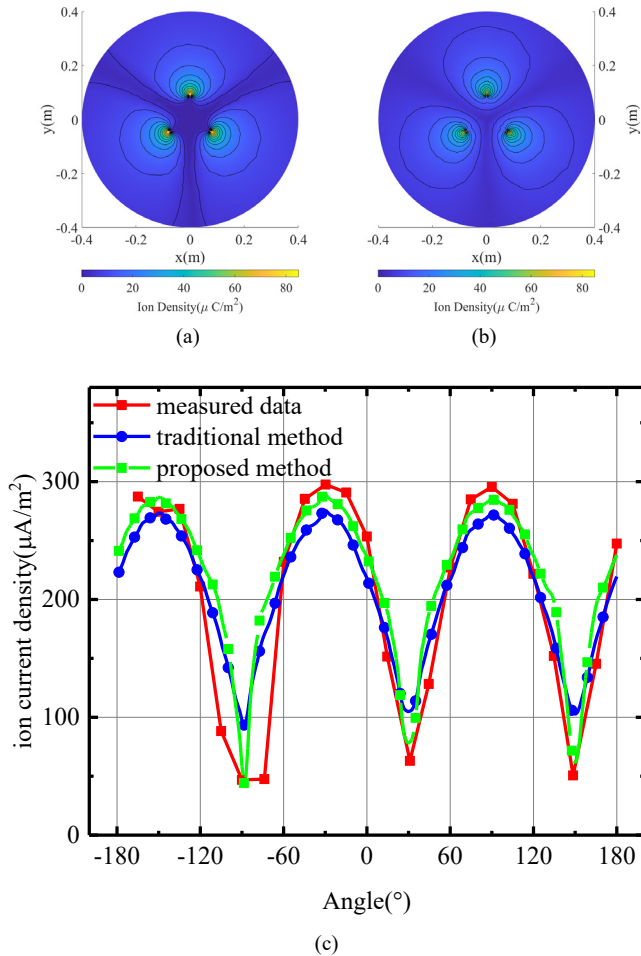Fig. 7. comparison of the ion density on the top conductor.

(a)

(b)

(c)

Fig. 8. (a) space charge distribution obtained by the proposed method with dynamic scheme. (b) space charge distribution obtained by the traditional mesh based method. (c)Measured and calculated corona current distribution around three split conductors.
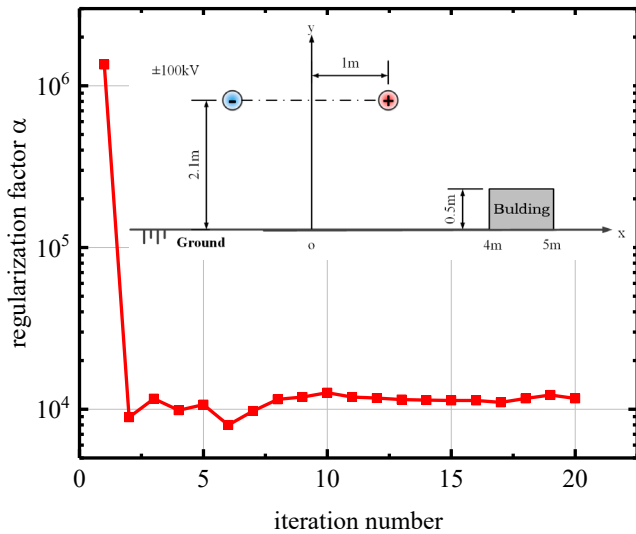

Fig. 9. the regularization factor α determined by the formula (33) during the iterations.
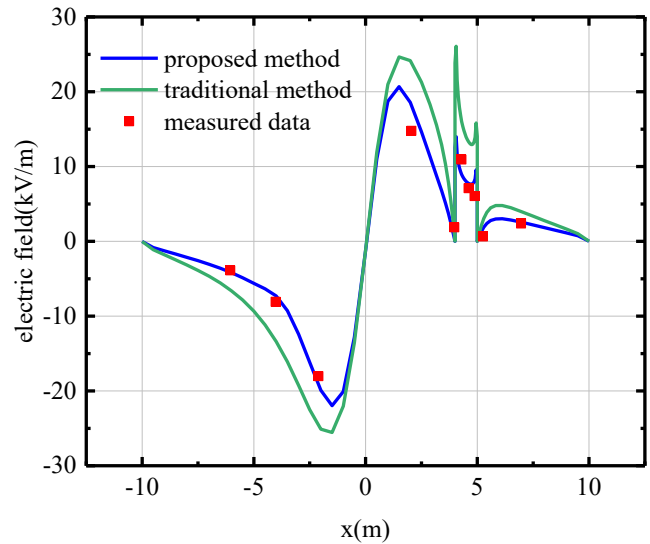

Fig.10. Measured and the calculated electric field on the ground and the top of the building.

[16] R.S. Sigmond, "The unipolar corona space charge flow problem", J. Eletrcostat. vol. 18, pp. 249-272, Feb. 1986.

[17] B. Chen, T. Lu and D. Wang, "Analysis of Ion flow field considering dielectric film under HVDC overhead transmission lines", IEEE Trans. Magn. vol. 56, no. 1, Jan. 2020.

[18] Y. Zhen, X. Cui, T. Lu, X. Li, C. Fang and X. Zhou, "3-D finite element method for calculating the ionized electric field and the ion current of the human body model under the UHVDC lines", IEEE Trans. Power Del. Vol. 28, no. 2, Apr. 2013.

[19] D. Wang, T. Lu, L. Hao, Q. Zhang, B. Chen and X. Li, "Calculation of ion-flow field near the crossing of HVDC transmission lines using equivalent corona conductors", IEEE Trans. Magn. vol. 55, no. 8, Aug. 2019.

[20] R. Tirumala, D. B. Go, "Comparative study of corona discharge simulation techniques for electrode configurations including non-uniform electric fields", J. Electrostat. vol. 72, pp. 99-106, 2014.

[21] Filamentary Ion Flow: theory and experiments, F. D. Lattarulo and V. Amoruso, Hoboken, New Jersey, USA: Wiley-IEEE Press, 2014.

[22] Elektrische Vorgange in Gasen und im Vacuum, N. A. Kapzow, Berlin: VEB Deutscher Verlag der Wissenschaften, 1955.

[23] K. Adamiak and P. Atten, "Simulation of corona discharge in point-plane configuration", J. Electrostat. vol. 61, pp. 85-98, Jan. 2004

[24] X. Zhou, X. Cui, T. Lu, C. Feng and Y. Zhan, "Spatial Distribution of Ion Current around HVDC bundle conductors", IEEE Trans. Power. Del. vol. 27, no. 1, pp. 380-390, Jan. 2012.

[25] X. Zhou, "Calculation Methods for Ion Flow Field from HVDC transmission lines parallel with HVAC transmission lines and its applications." Ph.D. dissertation, school of electric and electronic engineering, North China Electric Power University, China, 2013.

[26] Linear and Nonlinear Inverse Problems with Practical Applications, J. L. Muller and S. Siltanen, Society for industrial and Applied Mathematics 2012

[27] Matrix Analysis, R. A. Horn and C. R. Johnson, Cambridge, New York, Cambridge University Press, 2013.

[28] Z. Luo, X. Cui, W. Zhang and J. Lu, "Calculation of the 3D Ionized Field under HVDC transmission lines", IEEE Trans. Mag. vol. 47, no. 5, May, 2011.

[29] P. M. van den Berg and R. E. Leinmann, "A contrast source inversion method", Inverse Problem, vol .13, 1997.

Qiwen Cheng was born in Wuhan city of Hubei province in China in Dec. 1996. He received the B.Sc. degree in electrical engineering from Tsinghua University, Beijing, China, in 2018, where he is currently a Ph.D. student in the Department of

Electrical Engineering. His main research interest is computational electromagnetics.
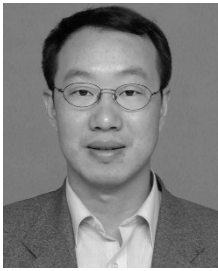
Jun Zou was born in Wuhan city of Hubei province in China in Jan. 1971. He received his B.S. and M.S. degrees from Zhengzhou University, Zhengzhou, China, in 1994 and 1997 respectively, and a Ph.D. degree from Tsinghua University, Beijing, China, in 2001, all in electrical engineering. In 2001, he joined electrical engineering department of Tsinghua University as an assistant researcher. In 2011, he was promoted to be a full professor. Dr. Jun Zou has been involving in researches on EMC in power systems, computational electromagnetics.

Stéphane Clénet was born in Nantes city in France in Apr. 1967. After the completion of his PhD, he was Assistant Professor at the University of Lille in 1994 before being appointed in 2002 as full professor of electrical engineering at Ecole Nationale Supérieure d'Arts et Métiers (ENSAM), France. In 2008, he was visiting professor as Fulbright Grantee at the University of Akron (USA) in 2008 and 2014 and at Mc Gill University (Canada) in 2015. He is working in the field of computational electromagnetics and its applications.